Program Digest, 2019 IEEE International Ultrasonics Symposium (IUS)
Glasgow, Scotland, October 6-9, 2019

Viscoelastic Response Ultrasound Detects Changes in Degree of Mechanical Anisotropy with Renal Fibrosis in Pig Model

*Md Murad Hossain[1], Timothy C. Nichols[2,3], Elizabeth P. Merricks[3], Dwight A. Bellinger[4], Lauren E. Wimsey[4], Melissa C. Caughey[2], Stephanie A. Montgomery[3], Caterina M. Gallippi[1]

[1]Joint Department of Biomedical Engineering, University of North Carolina at Chapel Hill, Chapel Hill and North Carolina State University, Raleigh, NC, USA,
[2]Department of Medicine, University of North Carolina at Chapel Hill, Chapel Hill, NC, USA,
[3]Department of Pathology and Laboratory Medicine, University of North Carolina at Chapel Hill, Chapel Hill, NC, USA,
[4]Department of Laboratory Animal Medicine, University of North Carolina at Chapel Hill, Chapel Hill, NC, USA.

***Abstract*— Chronic kidney disease is associated with progressive inflammation and fibrosis, which is conventionally assessed by invasive biopsy. A noninvasive alternative to biopsy may be interrogating elastic and viscous anisotropy. This work evaluates the feasibility of using *in vivo* Viscoelastic Response (VisR) ultrasound for detecting changes in the elastic and viscous degree of anisotropy (DoA) associated with fibrosis after chronic ischemia-reperfusion injury (IRI) in pig kidney. Histology was used to validate VisR DoA measurements, which were compared to those derived using Shear Wave Elasticity Imaging (SWEI) and Shearwave Dispersion Ultrasound Vibrometry (SDUV). In the injured and contralateral (control) kidneys of 8 pigs, VisR, SWEI, and SDUV-derived elastic DoA, evaluated as the ratio of longitudinal over transverse shear elasticity, was significantly ($p<0.1$, Wilcox Ranksum) decreased in the fibrotic medulla and increased in fibrotic cortex relative to control. Sirius red stain confirmed a significant ($p<0.1$, Wilcox Ranksum) increase in collagen content in the fibrotic medulla and cortex relative to control. These results suggest that VisR noninvasively detects changes in elastic DoA associated with fibrosis induced by chronic IRI in a pig model. VisR may be diagnostically relevant to delineating fibrosis in human kidney.**

Keywords— Renal inflammation; Chronic Kidney Disease; Anisotropy; VisR; ARFI; SWEI; SDUV.

I. Introduction

Fifteen percent of American adults, more than 30 million people, have chronic kidney disease (CKD). The symptoms of CKD start silently, progress through renal dysfunction, and terminate in end-stage renal disease (ESRD). Patients who are in the advanced state of ESRD are most desirably and cost-effectively treated by renal transplantation [1]. Although transplant surgery techniques and post-operative care have greatly advanced, death-censored graft survival is 74% [2]. Graft life could be extended by methods that support early identification of graft dysfunction. Current graft assessment methods include noninvasive, surrogate biomarkers like serum creatinine and proteinuria. However, these biomarkers lack sensitivity and specificity. In the absence of reliable surrogate biomarkers, some transplant programs implement surveillance or 'protocol' biopsies. However, biopsies are associated with bleeding complications and, in rare cases, transplant loss. A noninvasive, sensitive, and specific measure of renal allograft dysfunction is needed to enable timely intervention and prolong graft life.

Relevant biomarkers for monitoring renal allograft status are persistent allograft inflammation and progressive interstitial fibrosis [3]. Renal inflammation and fibrosis can be detected by interrogating the associated mechanical property alterations. Ultrasound-based mechanical property measurement methods, like compression elastography [4], transient elastography [5], and Acoustic Radiation Force Impulse (ARFI) imaging [6]–[8], have been applied to determine if parenchymal stiffness is correlated to fibrosis extent, but results were inconsistent. The variable findings may be due to the anisotropic nature of the renal parenchyma, in which elasticity is higher along versus across nephron alignment [9]. Exploiting elastic anisotropy in the renal parenchyma, and its changes with pathology, may be diagnostically relevant.

Recently, Hossain *et. al* developed a novel method to assess degree of anisotropy (DoA) in elasticity as the ratio of ARFI-induced peak displacements (PD) achieved when the long axis of a geometrically asymmetric ARFI excitation point spread function (PSF) was aligned along versus across the axis of symmetry (AoS) in simulated TI materials [10], [11]. The investigators applied this method to assess the mechanical anisotropy of renal cortex by orienting the ARFI excitation PSF long axis along versus across nephrons [12], [13]. However, renal tissue is viscoelastic [14], and if not properly considered, viscosity can corrupt elasticity assessment by PD. Rather than PD, Viscoelastic Response (VisR) ultrasound-derived relative elasticity (RE) has been shown to reflect tissue elasticity and separately from viscosity [15]–[17]. Thus, ratios of VisR-derived RE can be used to assess elastic DoA in renal parenchyma. We have previously shown that VisR-derived DoA increases with renal inflammation in a pig model of acute renal ischemia-reperfusion injury (IRI) [18]. The objective of this work is to evaluate the relevance of *in vivo* VisR-derived elastic DoA for detecting renal fibrosis in a pig model of chronic renal IRI.

II. Materials and Methods

A. Animal Experiments

Renal fibrosis was induced in either the left or right kidney of each pig using the IRI model. Pigs were sedated with 3.0 ml telazol and then fitted with a nose cone for the administration of

* Md Murad Hossain is now a post-doctoral research scientist at Columbia University.

inhaled isoflurane (4-5%) to induce anesthesia. An ear vein catheter was introduced for saline infusions (5 mL/min). To induce ischemia, the femoral artery was cut, and a balloon catheter was placed. The catheter was guided under fluoroscopy to the renal artery where a balloon was inflated to achieve occlusion. Full renal artery occlusion, confirmed by fluoroscopy, was maintained for 3 hours, after which the balloon was deflated, the catheter removed, and the kidney allowed to re-perfuse. Blood was drawn to measure serum biomarkers at 30 minutes before IRI as well as at 30 minutes and 1, 3, 7, 14, 30, 45, 60, 75, and 90 days after the start of reperfusion. Thirty minutes after the blood draw on day 90, the VisR, SWEI, and SDUV measurements were performed on both injured and contralateral control kidneys that were surgically exteriorized. After imaging, the kidneys were harvested for histological validation.

B. VisR, SWEI, and SDUV Data Acquisition

VisR, SWEI, and SDUV measurements were performed using a Siemens S3000 Helix imaging system equipped for research purposes and a 9L4 1.5D array transducer (Siemens Healthineers, Ultrasound Division, Issaquah, WA, USA). The imaging parameters employed for VisR, SWEI, and SDUV are listed in Table I. VisR ensembles consisted of two reference pulses, 2 ARF impulses, and 60 tracking pulses for ARF induced displacement monitoring. The separation between the two ARF excitations was 0.8 ms. The lateral field of view (FOV) was 2 cm, with 40 evenly spaced lateral lines.

SWEI and SDUV ensembles consisted of two reference pulses, 1 and 4 ARF impulses, and 70 and 530 tracking pulses, respectively. The location of the ARF excitation was held constant while the location of tracking beams varied across the FOV. The ARF excitation was repeated 25 (SWEI) and 16 (SDUV) times at the same lateral location, and tissue motion was tracked at 25 (SWEI) and 16 (SDUV) lateral locations ranging from 0 to 10 mm (SWEI) and 0.5 to 8.0 mm (SDUV) from the push location. For SDUV, the push beam consisted of four 300-cycle ARF excitations, repeated with a pulse repetition of 100 Hz. Two separate SWEI and SDUV acquisitions were acquired by varying the lateral location of the ARF excitations to span both medulla and cortex.

For DoA assessments in the medulla and cortex, data were acquired first with the short axis of the ARF PSF aligned along nephrons and then with the transducer manually rotated 90^o on its center axis such that the ARF PSF was aligned across nephrons. Figure 1(a) shows transducer positioning during data acquisitions. The imaging focal depth was maintained at 23 mm for all pigs and orientations by using acoustic standoff pads (AquaFlex, Civco, Iowa, USA).

C. VisR, SWEI, and SDUV Data Processing

Raw RF data from VisR, SWEI, and SDUV acquisitions were transferred from the scanner to a computational workstation for custom analysis. The ARF-induced motion was measured using one-dimensional axial normalized cross-correlation (NNC) [19] with a 376-μm (2λ, λ= wavelength) kernel length and an 80-μm search region.

TABLE I : IMAGING PARAMETERS.

Parameters	VisR/SWEI/SDUV
Transducer	9L4
Bandwidth	55.38%
Sampling freq.	40 MHz
ARF excitation duration	300 cycle
ARF excitation center frequency	4.0 MHz
ARF excitation F/#	1.5
ARF axial focus	23 mm
Tracking center frequency	6.0 MHz
Tracking transmit F/#	1.5
Tracking receive F/#*	0.75
Tracking transmit axial focus	23 mm
Acoustic lens focus (axial, lateral, elevation)	(23, 0, 0)
Tracking PRF	12.8 KHz

* Aperture growth and dynamic Rx focusing enabled

For VisR imaging, the resulting displacement profiles were fit to the mass-spring-damper model via a custom C++ implementation of the Nelder-Mead algorithm to derived RE and RV, which were rendered into 2D parametric images. In addition to RE and RV, PD was measured from each displacement profile and rendered into 2D images.

For SWEI, directional filtering [20] was applied to ARF-induced displacements to remove shear wave reflections. Then, for SWEI, shear wave velocity (SWV) was calculated using the method described in [21] in lateral sliding windows of 2.5 mm length. Shear modulus was estimated from the SWV (V) as, $\mu = \rho V^2$, where ρ is the density, assumed to be 1,000 kgm^{-3}. SDUV data were processed using the methods developed by Chen *et al.* [22] to derive material shear (μ_1) and viscous (μ_2) moduli. SDUV processing was performed using a lateral sliding window with dimension 3.0 mm. The two SWEI and SDUV acquisitions with different ARF excitation locations were combined to generate a single image of SWEI or SDUV derived shear modulus.

To assess DoA using VisR, SWEI, and SDUV, ROIs with dimensions 2.5 x 3.0 mm (axial x lateral) were selected in all images. The ROIs were positioned axially between 1.0 mm below and 1.5 mm above the focal depth. The lateral center of the ROI was approximately centered in the lateral FOV. Then, the median parameter value in each ROI was measured, and DoA was evaluated as the ratio of median parameter values obtained in the longitudinal versus transverse ARF PSF orientations. The paired Wilcoxon rank test [23] was used to statistically compare between outcomes in IRI versus control kidneys.

III. RESULTS AND DISCUSSION

In a representative *in vivo* control kidney, Figure 1(b-c) shows VisR-derived RE images of medulla acquired with the ARF short-axis aligned along and across nephrons, respectively. Note that RE predominately reflects the longitudinal shear elastic modulus when the ARF short axis is aligned along, and the transverse shear elastic modulus when the ARF short axis is aligned across, nephrons. Median RE in the ROI was 58.5 and

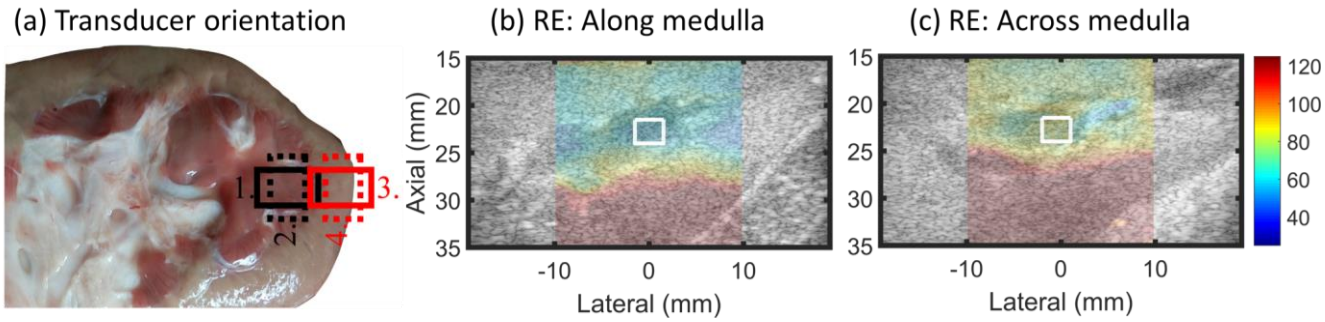

Figure 1: In a representative control kidney, (a) approximate transducer position (boxes) for imaging medulla (black) and cortex (red). Solid and dashed lines represent transducer orientations when the ARF short axis was aligned along and across nephrons, respectively. Numbers near the boxes indicate the order of data acquisition. (b-c) VisR derived RE images of the control medulla obtained with the ARF short axis aligned along (b) and across (c) nephrons. VisR images are overlaid with transparency on the matched B-modes for anatomical reference. White contours indicate measurement regions of interest.

80.2 mm^{-1} in along and across nephron alignments, respectively, for a shear elastic DoA of 58.5/80.2 = 0.73.

After IRI, serum creatinine was significantly higher than at baseline ($p < 0.05$), which suggest declining kidney function. Figure 2 shows representative Sirius Red stains of control and IRI cortex. The IRI cortex is marked by the presence of higher collagen fiber content (red in the stain) between tubules and glomeruli. Quantitative analyses showed a significant increase (Wilcoxon, $p<0.05$) in collagen area in IRI versus control medulla and cortex.

Associated with the observed fibrosis following IRI, Table II shows that VisR RE and PD, SWEI μ, and SDUV μ_1 indicate decreased DoA in IRI medulla and increased DoA in IRI cortex compared to control. Increased DoA in the cortex was mostly attributed to decreased transverse and increased longitudinal shear elastic moduli, whereas decrease DoA in medulla was mainly due to decreased longitudinal modulus. VisR RV indicates decreased viscous DoA in the IRI medulla.

One limitation of the described experimental design is the potential for misalignment of measurements intended to be made across or along nephrons. The transducer was positioned manually using only B-mode guidance, and nephron orientation was not always clearly visible. If the transducer was not properly aligned along or across nephrons, the associated DoA measures would have been artifactually reduced. Another limitation is that the contralateral control kidneys may have experienced some tissue damage due to the exteriorization process. Despite these limitations, this study demonstrates that VisR imaging delineates changes in mechanical DoA that are associated with kidney fibrosis induced by IRI.

IV. Conclusion

This study demonstrates the feasibility of using *in vivo* VisR derived mechanical DoA for detecting fibrosis associated with IRI in a pig model. Histology confirmed kidney fibrosis following IRI. VisR detected significantly lower elastic DoA in IRI medulla and higher DoA in IRI cortex, which was corroborated by SWEI and SDUV derived elastic DoA. VisR derived RV indicated decreased viscous DoA in IRI medulla. These results show that VisR noninvasively detects changes in

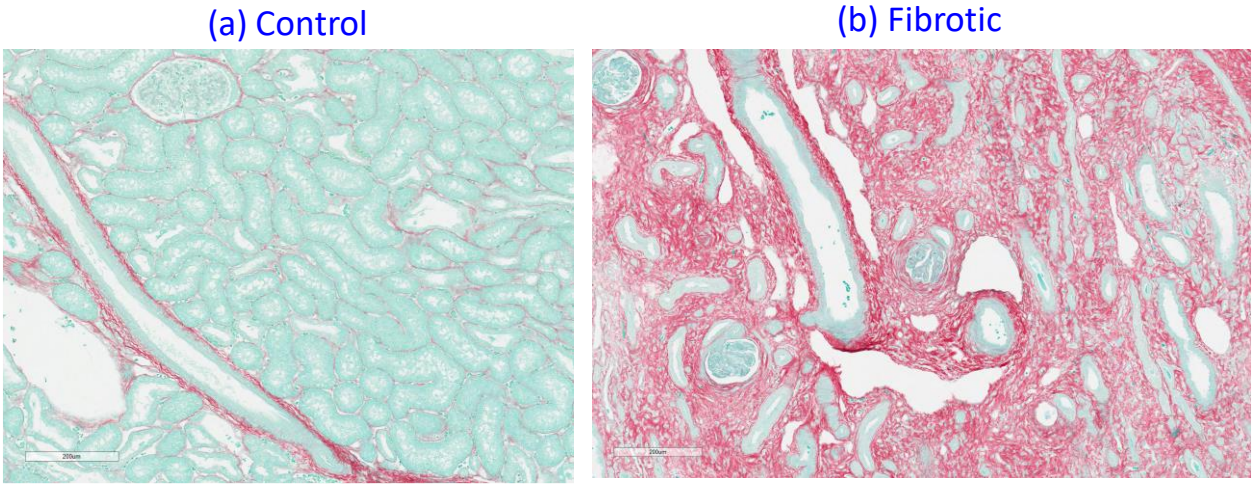

Figure 2: Representative Sirius Red stains of (a) control and (b) fibrotic cortex. The fibrotic cortex is marked by the presence of higher collagen fiber content (red stain) between tubules and glomeruli.

Table II: VisR, SWEI, and SDUV derived DoA measured in the medulla and cortex. Significant difference between fibrotic and control cases are shown by asterisk (* and ** represent $p < 0.1$ and $p < 0.05$, respectively).

DoA Types	Imaging Parameters	Medulla		Cortex	
		Control	Fibrotic	Control	Fibrotic
Elastic	VisR: RE (1/mm)	**0.98±0.14**	**0.82±0.05****	**1.01±0.17**	**1.36±0.30***
	VisR: PD (μm)	**1.01±0.09**	**0.83±0.08****	**0.96±0.17**	**1.37±0.25***
	SWEI : μ (KPa)	**0.89±0.08**	**0.61±0.09****	1.11±0.09	1.31±0.28
	SDUV: μ_1 (KPa)	**0.87±0.17**	**0.57±0.12***	**1.03±0.20**	**1.54±0.47***
Viscous	VisR: RV(ms/mm)	**1.06±0.19**	**0.69±0.20***	0.92±0.421	0.75±0.32
	SDUV: μ_2 (Pa.s)	1.37±1.32	2.74±2.23	1.48±1.41	0.44±0.44

elastic and viscous DoA associated with fibrosis following IRI in a pig model. VisR-derived mechanical DoA may be diagnostically relevant to noninvasively delineating fibrosis in human kidneys, *in vivo*.

ACKNOWLEDGMENT

The authors thank the physicians and staff in the Francis Owen Blood Research Lab, UNC. The authors also thank Siemens Healthcare, Ultrasound Division, Issaquah, WA, USA. Funding for this work was from NIH grants R01DK107740, R01NS074057, and R01HL092944.

REFERENCES

[1] M. Abecassis *et al.*, "Kidney transplantation as primary therapy for end-stage renal disease: A National Kidney Foundation/Kidney Disease Outcomes Quality Initiative (NKF/KDOQI™) conference," *Clin. J. Am. Soc. Nephrol.*, vol. 3, no. 2, pp. 471–480, 2008.

[2] M. D. Stegall, L. D. Cornell, W. D. Park, B. H. Smith, and F. G. Cosio, "Renal Allograft Histology at 10 Years After Transplantation in the Tacrolimus Era: Evidence of Pervasive Chronic Injury.," *Am. J. Transplant*, vol. 18, no. 1, pp. 180–188, Jan. 2018.

[3] M. Gago, L. D. Cornell, W. K. Kremers, M. D. Stegall, and F. G. Cosio, "Kidney allograft inflammation and fibrosis, causes and consequences," *Am. J. Transplant.*, vol. 12, no. 5, pp. 1199–1207, 2012.

[4] J. Gao and J. M. Rubin, "Ultrasound strain zero-crossing elasticity measurement in assessment of renal allograft cortical hardness: a preliminary observation.," *Ultrasound Med. Biol.*, vol. 40, no. 9, pp. 2048–57, Sep. 2014.

[5] C. Sommerer *et al.*, "Assessment of renal allograft fibrosis by transient elastography," *Transpl. Int.*, vol. 26, no. 5, pp. 545–551, 2013.

[6] K. F. Stock *et al.*, "ARFI-based tissue elasticity quantification and kidney graft dysfunction: First clinical experiences," *Clin. Hemorheol. Microcirc.*, vol. 49, no. 1–4, pp. 527–535, 2011.

[7] T. Syversveen, K. Midtvedt, A. E. Berstad, K. Brabrand, E. H. Strøm, and A. Abildgaard, "Tissue elasticity estimated by acoustic radiation force impulse quantification depends on the applied transducer force: an experimental study in kidney transplant patients.," *Eur. Radiol.*, vol. 22, no. 10, pp. 2130–7, Oct. 2012.

[8] M. M. Hossain *et al.*, "Evaluating Renal Transplant Status Using Viscoelastic Response (VisR) Ultrasound.," *Ultrasound Med. Biol.*, vol. 44, no. 8, pp. 1573–1584, May 2018.

[9] J.-L. Gennisson, N. Grenier, C. Combe, and M. Tanter, "Supersonic shear wave elastography of in vivo pig kidney: influence of blood pressure, urinary pressure and tissue anisotropy.," *Ultrasound Med. Biol.*, vol. 38, no. 9, pp. 1559–67, Sep. 2012.

[10] M. M. Hossain and C. M. Gallippi, "Estimation of degree of anisotropy in transversely isotropic (TI) elastic materials from Acoustic Radiation Force (ARF)-induced peak displacements," in *2015 IEEE International Ultrasonics Symposium (IUS)*, 2015, pp. 1–4.

[11] M. M. Hossain, C. J. Moore, and C. M. Gallippi, "Acoustic Radiation Force Impulse (ARFI)-Induced Peak Displacements Reflect Degree of Anisotropy in Transversely Isotropic Elastic Materials.," *IEEE Trans. Ultrason. Ferroelectr. Freq. Control*, vol. 64, no. 6, pp. 989–1001, May 2017.

[12] M. M. Hossain *et al.*, "In vivo mechanical anisotropy assessment in renal cortex using ARFI peak displacement," in *2017 IEEE International Ultrasonics Symposium (IUS)*, 2017, vol. 64, no. 6, pp. 1–4.

[13] M. Hossain *et al.*, "Mechanical Anisotropy Assessment in Kidney Cortex Using ARFI Peak Displacement: Preclinical Validation and Pilot In Vivo Clinical Results in Kidney Allografts," *IEEE Trans. Ultrason. Ferroelectr. Freq. Control*, no. In Press, 2018.

[14] C. Amador, M. Urban, and R. Kinnick, "In vivo swine kidney viscoelasticity during acute gradual decrease in renal blood flow: pilot study," *Rev. Ing. …*, vol. 7, no. 13, pp. 68–78, 2013.

[15] M. R. Selzo, C. J. Moore, M. M. Hossain, M. L. Palmeri, and C. M. Gallippi, "On the Quantitative Potential of Viscoelastic Response (VisR) Ultrasound Using the One-Dimensional Mass-Spring-Damper Model.," *IEEE Trans. Ultrason. Ferroelectr. Freq. Control*, vol. 63, no. 9, pp. 1276–87, Sep. 2016.

[16] M. M. Hossain, T. Nichols, E. Merricks, and C. Gallippi, "Viscoelastic response (VisR)-derived relative elasticity and relative viscosity reflect tissue elasticity and viscosity: In silico and experimental demonstration in liver," in *2017 IEEE International Ultrasonics Symposium (IUS)*, 2017, no. 2, pp. 1–1.

[17] M. Hossain, C. Moore, and C. Gallippi, "On the quantitative potential of Viscoelastic Response (VisR) ultrasound using matrix array transducers: In silico demonstration," in *2016 IEEE International Ultrasonics Symposium (IUS)*, 2016, vol. 3010, no. c, pp. 1–4.

[18] M. MuradHossain *et al.*, "Viscoelastic Response Ultrasound Detects Increased Degree of Mechanical Anisotropy with Ischemia-Reperfusion Injury in Pig Kidney, In Vivo," in *2018 IEEE International Ultrasonics Symposium (IUS)*, 2018, pp. 1–4.

[19] G. F. Pinton, J. J. Dahl, and G. E. Trahey, "Rapid tracking of small displacements with ultrasound.," *IEEE Trans. Ultrason. Ferroelectr. Freq. Control*, vol. 53, no. 6, pp. 1103–17, Jun. 2006.

[20] T. Deffieux, J. L. Gennisson, J. Bercoff, and M. Tanter, "On the effects of reflected waves in transient shear wave elastography," *IEEE Trans. Ultrason. Ferroelectr. Freq. Control*, vol. 58, no. 10, pp. 2032–2035, 2011.

[21] K. Nightingale, S. McAleavey, and G. Trahey, "Shear-wave generation using acoustic radiation force: in vivo and ex vivo results.," *Ultrasound Med. Biol.*, vol. 29, no. 12, pp. 1715–1723, Dec. 2003.

[22] S. Chen *et al.*, "Shearwave dispersion ultrasound vibrometry (SDUV) for measuring tissue elasticity and viscosity.," *IEEE Trans. Ultrason. Ferroelectr. Freq. Control*, vol. 56, no. 1, pp. 55–62, Jan. 2009.

[23] J. D. Gibbons and S. Chakraborti, *Nonparametric statistical inference*. Chapman & Hall/Taylor & Francis, 2011.